Thermochimica Acta, 20 (1977) 219–228

WEAK TRANSVERSE MAGNETIC FIELD EFFECT ON THE VISCOSITY OF $Mn(NO_3)_2$–H_2O SOLUTION AT SEVERAL TEMPERATURES

J. LIELMEZS AND H. ALEMAN
Chemical Engineering Department, The University of British Columbia, Vancouver, B.C. (Canada)
(Received 7 September 1976)

ABSTRACT

Experiments show that transversally applied magnetic field H of strength 12 kG at 10, 15, 20, 25, 30, 40 and 60°C and the ambient pressure decreases the viscosity of high concentration $Mn(NO_3)_2$–H_2O solution. The largest value of this decrease occurs at the temperature range of 20–25°C. On the other hand, at low paramagnetic ion concentrations, the applied magnetic field increases the viscosity of $Mn(NO_3)_2$–H_2O solution in such a way that the observed effect value in the limit seems to approach the already measured viscosity increase of the pure water. However, the temperature dependence of the observed viscosity increase of the given dilute paramagnetic $Mn(NO_3)_2$–H_2O solution appears to be more complex and at some temperatures even opposite to that of the already shown viscosity–temperature behavior of the diamagnetic pure water.

INTRODUCTION

This work describes the applied transverse magnetic field effect on the viscosity of $Mn(NO_3)_2$–H_2O solution at 10, 15, 20, 25, 30, 40 and 60°C temperature (Table 1, Figs. 1–5). It was found that the applied magnetic field H of the strength of 12 kG at high paramagnetic salt concentrations decreases the viscosity of $Mn(NO_3)_2$–H_2O solution while at low salt concentrations the applied magnetic field increases the viscosity of this solution in such a way that the observed effect value appears to approach the already measured[1–4] viscosity increase of the pure diamagnetic water. However, the obtained results (Table 1, Figs. 1–5) show that the temperature dependence of the observed viscosity increase of the dilute $Mn(NO_3)_2$–H_2O solution seems to be more complex and at some temperatures (10–20°C range) even opposite to the already shown[1, 2] viscosity–temperature behavior of the pure water under the influence of an applied external magnetic field. Indeed these complex, low temperature, dilute solutions (the paramagnetic ion solution approaches at the infinite dilution the diamagnetic pure water) might specify[1, 2, 4] the existence of two competing microstructural interaction mechanisms, the dipolar interaction associated with the pure water; and the spin-exchange mechanism characterizing the paramagnetic ion–water

TABLE 1

SUMMARY OF RESULTS[a]

Temp. °C	*0.005 Molar conc. Arithmetical mean average viscosity* $\nu^* = \frac{\nu^{II} - \nu^0}{\nu^0} \times 100$	*Statistical analysis Standard deviation*[b] σ_{II}	*Null hypothesis with*[c] $\mu_{II} = \mu_0$ $\sigma_{II} \neq \sigma_0$	*0.5 Molar conc. Arithmetical mean average viscosity* $\nu^* = \frac{\nu^{II} - \nu^0}{\nu^0} \times 100$	*Statistical analysis Standard deviation*[b] σ_{II}	*Null hypothesis with*[c] $\mu_{II} = \mu_0$ $\sigma_{II} \neq \sigma_0$
10	+ 0.0245	4.4136×10^{-4}	Rejects at 90% confidence level	− 1.0279	8.5323×10^{-4}	Rejects at 99% confidence level
15	+ 0.2031	1.4142×10^{-4}	Rejects at 95% confidence level	− 1.0475	5.0498×10^{-4}	Rejects at 99% confidence level
20	+ 0.1250	4.3216×10^{-4}	Rejects at 90% confidence level	− 1.0102	2.1213×10^{-4}	Rejects at 95% confidence level
25	+ 0.1200	3.7859×10^{-4}	Rejects at 90% confidence level	− 1.2924	1.6432×10^{-4}	Rejects at 95% confidence level
30	+ 0.1882	4.8990×10^{-4}	Rejects at 90% confidence level	− 1.0327	0.0000	Rejects at 95% confidence level
40	+ 0.0470	1.9494×10^{-4}	Does not reject.	− 1.0264	3.4928×10^{-4}	Rejects at 95% confidence level
60	+ 0.0728	1.1691×10^{-4}	Rejects at 90% confidence level	0.9511	2.6395×10^{-4}	Rejects at 95% confidence level

Temp. °C	*1 Molar conc. Arithmetical mean average viscosity* $\nu^* = \frac{\nu^{II} - \nu^0}{\nu^0} \times 100$	*Statistical analysis Standard deviation*[b] σ_{II}	*Null hypothesis with*[c] $\mu_{II} = \mu_0$ $\sigma_{II} \neq \sigma_0$	*3 Molar conc. Arithmetical mean average viscosity* $\nu^* = \frac{\nu^{II} - \nu^0}{\nu^0} \times 100$	*Statistical analysis Standard deviation*[b] σ_{II}	*Null hypothesis with*[c] $\mu_{II} = \mu_0$ $\sigma_{II} \neq \sigma_0$
10	− 2.5243	1.0050×10^{-3}	Rejects at 99% confidence level	− 6.6058	2.2488×10^{-3}	Rejects at 99% confidence level
15	− 2.4655	4.9193×10^{-4}	Rejects at 99% confidence level	− 6.4124	1.5232×10^{-3}	Rejects at 99% confidence level
20	− 2.4850	2.6077×10^{-4}	Rejects at 99% confidence level	− 6.4364	1.2377×10^{-3}	Rejects at 99% confidence level
25	− 2.6208	6.8044×10^{-4}	Rejects at 99% confidence level	− 6.1543	6.8191×10^{-4}	Rejects at 99% confidence level
30	− 2.3297	2.5884×10^{-4}	Rejects at 99% confidence level	− 5.9567	1.0886×10^{-4}	Rejects at 99% confidence level
40	− 2.2634	9.8336×10^{-4}	Rejects at 99% confidence level	5.7998	1.0985×10^{-4}	Rejects at 99% confidence level
60	− 2.1836	1.6432×10^{-4}	Rejects at 90% confidence level	5.3711	4.3932×10^{-4}	Rejects at 99% confidence level

[a] For detailed discussion regarding the use of statistical analysis methods, see any appropriate standard textbook.

[b] Standard deviation σ_x is defined as: $\sigma_x = \sqrt{\frac{\sum_{i=1}^{n} (X_i - \bar{X})^2}{n-1}}$

[c] To test t-distribution null-hypothesis, it was assumed that true mean $\mu_{II} = \mu_0$, while the variances, $\sigma_{II} \neq \sigma_0$.

solution. Additionally to this, these experiments strongly support the recent findings of Lielmezs et al.[1] and Lielmezs and Aleman[2] that an externally applied magnetic field weakly increases the viscosity of pure distilled water.

EXPERIMENTAL

Lielmezs and co-workers[1–4] describe in detail the apparatus and methods used for the measurement and evaluation of the transverse applied magnetic field on the viscosity of pure distilled water and of paramagnetic ion–water solutions. The measuring apparatus[1–4] consists of two parts: the electromagnet system and the viscometer–temperature bath assembly. The same Cannon–Fenske opaque (calibrated, reverse flow, No. 50, V 561) viscometer was retained for use in this work; and the same viscometer cleaning and measurement procedures as well as calculation methods were used in this work. Consequently, the overall accuracy of this study is at the same level as found and in detail discussed in our previous work[1–4]. To prepare the $Mn(NO_3)_2$–H_2O solutions, 50% analytical reagent grade $Mn(NO_3)_2$ from Mallinckrodt Chemical Works, was used.

RESULTS AND DISCUSSION

The viscosities of $Mn(NO_3)_2$–H_2O solution for both the applied and the not applied (ambient earth magnetic field) magnetic field condition were calculated from the simplified[1–4] relation:

$$\nu = Ct \tag{1}$$

where: ν = viscosity in stokes; C = constant (determined by calibration); t = efflux time in seconds.

The results of this study are summarized in Table 1 and Figs. 1–5. Table 1 presents at 10, 15, 20, 25, 30, 40 and 60°C temperature for all solution concentrations, at the magnetic field strength $H = 12$ kG; the fractional viscosity coefficient, defined as $\nu^* = [(\nu^H - \nu^0)/\nu^0] \times 100$; where ν^H is the arithmetic mean average viscosity of the given solution at the 25°C temperature, the atmospheric pressure and the applied magnetic field strength $H = 12$ kG. The ν^0, however, is the arithmetic mean average viscosity at the ambient earth magnetic field (or no-field condition) but at the same concentration, temperature and pressure as ν^H.

Table 1 also presents statistical analysis data; standard deviation σ_H, calculated at the applied magnetic field strength H, and the t-distribution null-hypothesis results, assuming that the means are equal ($\mu_H = \mu_0$) while the variances for the applied field and the no-field conditions are not equal; that is, $\sigma_H \neq \sigma_0$.

The obtained results (Table 1, Figs. 1–5) show definite patterns between the involved parameters, the fractional viscosity, ν^*, the solution concentration, C(mol l^{-1}); and the measurement temperature T, at constant applied magnetic field strength of $H = 12$ kG. First, the $\nu^* - T$ plot (Fig. 1) shows that for all experimental

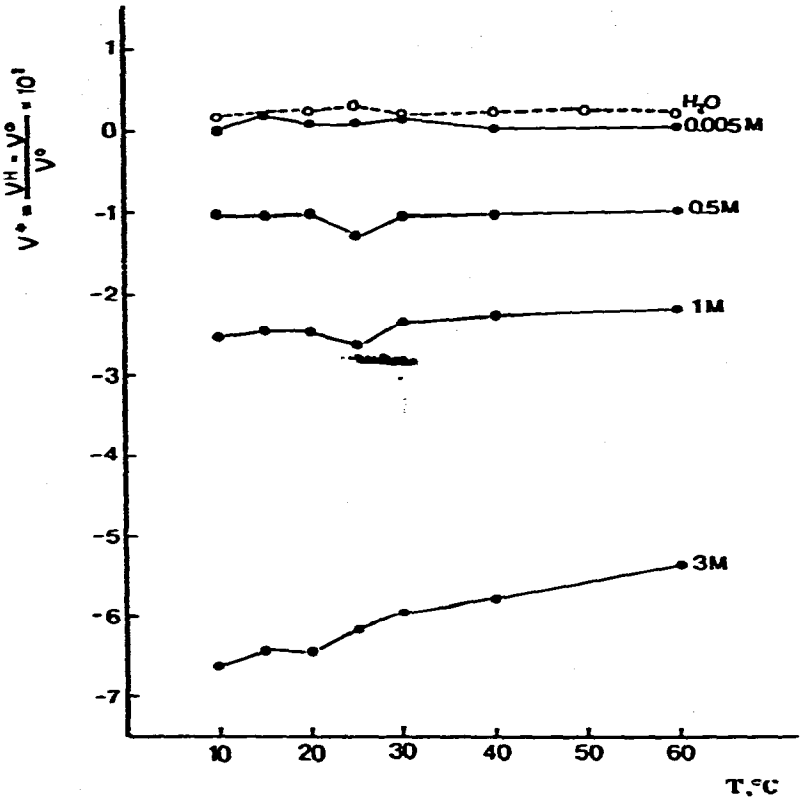

Fig. 1. The fractional viscosity v^* ($v^* = [v^H - v^0/v^0] \times 10^2$) and temperature T relation. The v^*-data for the pure liquid water were taken from ref. 2.

temperatures (10, 15, 20, 25, 30, 40 and 60°C), at all $Mn(NO_3)_2$–H_2O solution concentrations (0.005, 0.5, 1.0 and 3.0 mol l^{-1}), within the 17.5–30°C range there exists a downward $v^* - T$ value peak. However, as the paramagnetic nitrate solution becomes more dilute, this downward peak tends to become fainter and in the limit of an approaching infinite dilution, is only slightly diverging from the already established upward peak found in the v^*–T curve for the pure water[2, 4] (the v^*–T curve for the pure water is included as an upper limit in Fig. 1, this work). This analysis is further extended by Fig. 2, in which we have plotted $Mn(NO_3)_2$–H_2O solution fractional viscosity v^*–difference (Δv^*) and the corresponding temperature T–difference (ΔT) ratio taken at constant concentration of the solution against the temperature T in °C (values obtained from Table 1, this work). Figure 2 confirms that indeed the fractional viscosity v^*–temperature coefficient for the $Mn(NO_3)_2$–H_2O solution may suddenly change the sign; and that this change of sign appears to be opposite to the observed sign of change of the pure water[2, 4] at the same temperature range. As a matter of fact, the Arrhenius plot (Fig. 3) of the absolute values of the fractional viscosity v^* of $Mn(NO_3)_2$–H_2O solution (Table 1) indicates the presence of discontinuous structural rearrangements occurring in the solution between the 17.5 to 30°C temperature range for 0.5, 1.0 and 3.0 mol l^{-1} concentrations and

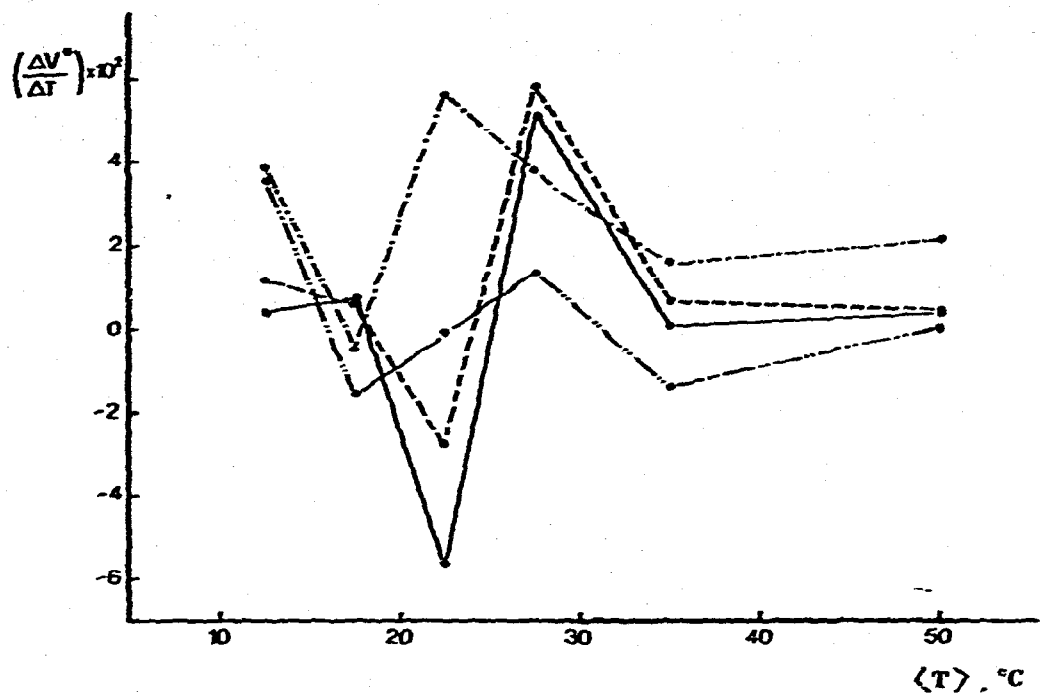

Fig. 2. The fractional viscosity–temperature coefficient ($[\Delta\nu^*/\Delta T] \times 10^2$) and the average temperature $\langle T\rangle$ ($\langle T\rangle = (T_1 + T_2)/2$) relation with respect to state (1) and state (2).

between the 15 to 35°C range for 0.005 mol l^{-1} solution. It is of interest to note that when the $Mn(NO_3)_2$–H_2O solution activation energy curves are compared with the activation energy curve for the pure water[2] (included also in Fig. 3); then within the accuracy of our measurements, the low concentration (0.005 mol l^{-1}) $Mn(NO_3)_2$–H_2O solution Arrhenius plot (note that these are the absolute fractional viscosity ν^*-values) displays the same behavioral patterns of liquid flow as that of the pure water. This also confirms our previous findings[3, 4] showing that for each of the following paramagnetic nitrate–water solutions: $Cu(NO_3)_2$–H_2O; $Ni(NO_3)_2$–H_2O; $Co(NO_3)_2$–H_2O and $Mn(NO_3)_2$–H_2O; there is a critical concentration, $\bar{C}_c$; at which the observed magnetic field effect on the solution viscosity changes its direction, that is, the decrease in ν^*-value now becomes an increase in the value of solution viscosity which in the limit of the infinite dilution of the solution, approaches the positive ν^*-value of the pure water. For the $Mn(NO_3)_2$–H_2O solution the critical concentration value was found[4] to be $\bar{C}_c = 0.065$ mol l^{-1}. The effect of the existence of this critical solution concentration on the ν^*–T curve is displayed by Fig. 1. It shows that above the critical concentration, $\bar{C}_c$; at 0.5, 1.0 and 3.0 mol l^{-1} concentrations, first, the slope of the ν^*–T decreases with decreasing concentration and becomes nearly zero at 0.5 mol l^{-1} concentration, while at the same time the downward peak temperature shifts from 20°C (at 3.0 mol l^{-1}) to 25°C (at 0.5 mol l^{-1}). The peak shapes also change: the downward peak becomes somewhat narrower as the concentration decreases.

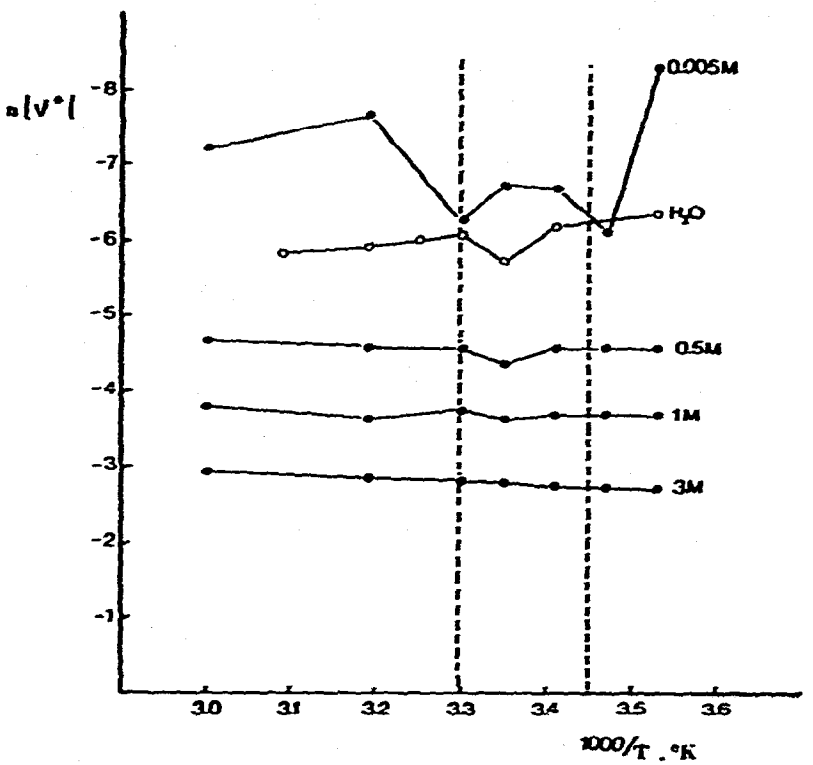

Fig. 3. The Arrhenius plot for the absolute fractional viscosity $\ln|\nu^*|$. To interpret the actual flow patterns of this Figure, recall that for the pure water and low concentration (below the critical solution concentration $\bar{C}_c$, ref. 4) paramagnetic nitrate–water solutions; the fractional viscosity ν^* increases while above the critical solution concentration ν^* decreases. The ν^*-data for the pure water are taken from ref. 2.

Second, below the critical solute concentration ($\bar{C}_c = 0.065$ mol l^{-1}) the ν^*-value confirming with our previous work[4] increases and in the limit tends to approach that of the pure water[3, 4]. On the other hand, the low concentration (0.005 mol l^{-1}) ν^*–T curve still retains the general features of the higher concentration value ν^*–T curves as shown by the peak temperatures of ν^*–T plot at the 0.005 mol l^{-1} concentration (Fig. 1). The maximum peak temperatures on the ν^*–T curve for this low concentration, however, are found at 15°C and at 30°C as opposed to the pure water for which the maximum peak temperature was found in the vicinity of 25°C temperature[2]. The 0.005 mol l^{-1} solution ν^*–T curve (Fig. 1) for the 25°C region shows a shallow minimum. This general flow behavior* is reflected in the activation energy curves (Fig. 3). The presented Arrhenius plots (Fig. 3) of the absolute values of the fractional viscosity ν^* indicate that at concentrations above the critical concentration,

* Andalaro et al.[5] while studying the microscopic properties of the pure water by means of IR-spectroscopy have observed structural anomalies in the temperature dependence of the 1.2-μ absorption band of liquid water within the 30–40°C temperature range. On the other hand, Peschel and Adlfinger[6] have found that the surface zone of water adjacent to a highly polar surface shows strong temperature dependency and changes structurally over relatively large distances.

$\bar{C}_c$ (0.5, 1.0 and 3.0 mol l^{-1}); the activation energy except for the pronounced discontinuous kink temperature region between 17.5 and 30°C, appears to be nearly constant. If this solution activation energy curve is compared with the activation energy curve of the pure water[2], it appears that under the influence of an applied magnetic field of 12 kG, the solution at the higher concentrations becomes structurally more stable. However, if the low concentration (below the critical concentration, $\bar{C}_c$) fractional viscosity coefficient is compared with the fractional viscosity coefficient of the pure water (Fig. 3); one finds that the bulk liquid possesses a highly unstable and complex structural rearrangement pattern. This seems strongly to support the previously made assertion by Lielmezs and Aleman[4] that paramagnetic nitrate–water solution interactions may be characterized by two competing microstructural mechanisms: the dipolar interaction mechanism, chiefly associated with the proton longitudinal (spin-lattice) relaxation times and determining the pure diamagnetic liquid water behavior; and the spin-exchange mechanism, mainly associated with the proton transverse (spin–spin) relaxation time and determining the paramagnetic ion–water solution behavior.

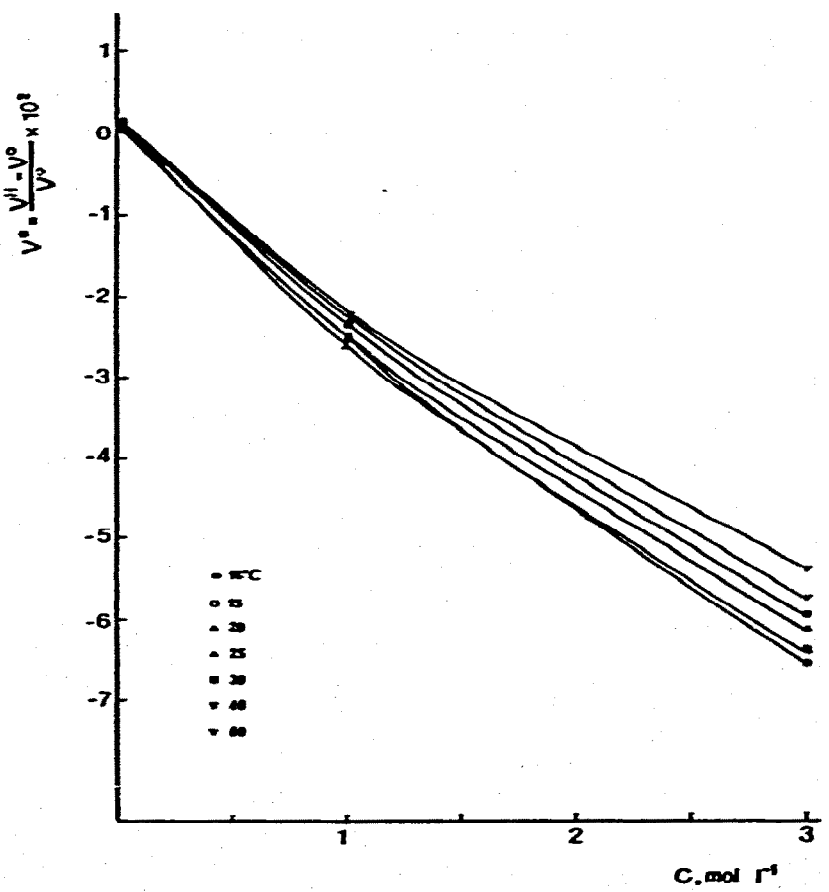

Fig. 4. The fractional viscosity ν^* and the paramagnetic $Mn(NO_3)$–H_2O solution concentration C plot.

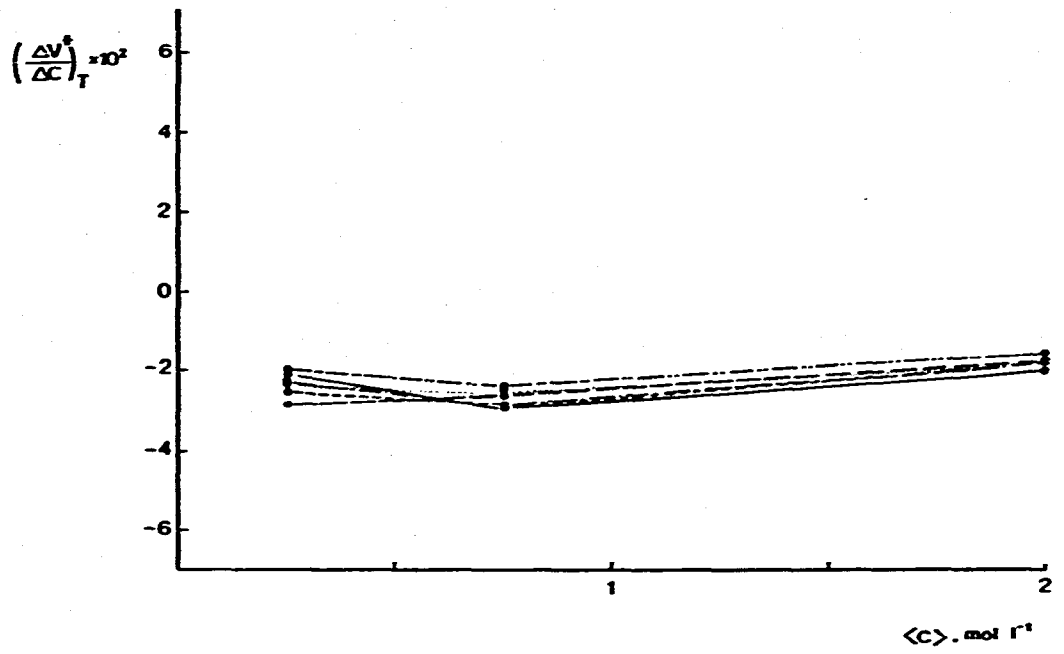

Fig. 5. The fractional viscosity–concentration coefficient ($[\Delta v^*/\Delta C] \times 10^2$) and the average concentration $\langle C \rangle$ plot with respect to state (1) and state (2); where $\langle C \rangle = (C_1 + C_2)/2$.

Figure 4 shows a smooth monotonic fractional viscosity v^* and concentration C plot. The v^*-value spread at higher concentrations is larger than at the lower concentrations. This may well be associated with the observation that in the limit of infinite dilution, the v^*-values for all temperatures tend to approach even if overlapping the corresponding v^*-value of the pure water. Comparing the results of Fig. 2 ($\Delta v^*/\Delta T$–$\langle T \rangle^*$ plot) with the results of Fig. 5 ($\Delta v^*/\Delta C$–$\langle C \rangle^{**}$ plot); it is seen that the slope of v^*–T curve (Fig. 1) when plotted against $\langle T \rangle$ suggests the existence of sudden, strong and temperature-dependent changes in the bulk structure (compare with Fig. 3) in the liquid.

In contrast, Fig. 5 shows that when the slope of the v^*–C curve (Fig. 4) is plotted against $\langle C \rangle$; the sudden strong, temperature dependent slope changes characterizing the v^*–T behavior; have vanished; but instead yielding only one gentle slope change in the vicinity of $\langle C \rangle = 0.75$ mol l^{-1}. This suggests that while the increased concentration of the paramagnetic $Mn(NO_3)_2$ ion increases the magnitude of the observed applied magnetic field effect on the solution viscosity (Fig. 4); the mechanism responsible for these v^*-value changes must be sought in the factors determining the structural stability of the liquid at the given thermodynamic (including the magnetic) state of the paramagnetic ion–diamagnetic water system.

---

* $\langle T \rangle = (T_1 + T_2)/2$.
** $\langle C \rangle = (C_1 + C_2)/2$.

ACKNOWLEDGEMENT

We gratefully acknowledge the financial assistance of the National Research Council of Canada.

REFERENCES

1 J. Lielmezs, H. Aleman and L. Fish, *Z. Phys. Chem., N. F.*, 99 (1976) 117.
2 J. Lielmezs and H. Aleman, *Thermochim. Acta*, 18 (1977) 315.
3 J. Lielmezs and H. Aleman, *Thermochim. Acta*, (1977) in press.
4 J. Lielmezs and H. Aleman, unpublished data.
5 G. Andaloro, M. B. Palma-Vittorelli and M. U. Palma, *J. Solut. Chem.*, 4 (1975) 215.
6 G. Peschel and K. H. Adlfinger, *Z. Naturforsch.*, 26 (1971) 707.